

Neural Quantum States of frustrated magnets: generalization and sign structure

Tom Westerhout,^{1,*} Nikita Astrakhantsev,^{2,3,4,†} Konstantin S. Tikhonov,^{5,6,7,‡} Mikhail I. Katsnelson,^{1,8,§} and Andrey A. Bagrov^{1,8,9,¶}

¹*Institute for Molecules and Materials, Radboud University, Heijendaalseweg 135, 6525 AJ, Nijmegen, The Netherlands*

²*Physik-Institut, Universität Zürich, Winterthurerstrasse 190, CH-8057 Zürich, Switzerland*

³*Moscow Institute of Physics and Technology, Institutsky lane 9, Dolgoprudny, Moscow region, 141700 Russia*

⁴*Institute for Theoretical and Experimental Physics NRC “Kurchatov Institute”, Moscow, 117218 Russia*

⁵*Institut für Nanotechnologie, Karlsruhe Institute of Technology, 76021 Karlsruhe, Germany*

⁶*Skolkovo Institute of Science and Technology, 143026 Skolkovo, Russia*

⁷*Landau Institute for Theoretical Physics RAS, 119334 Moscow, Russia*

⁸*Theoretical Physics and Applied Mathematics Department, Ural Federal University, 620002 Yekaterinburg, Russia*

⁹*Department of Physics and Astronomy, Uppsala University, Box 516, SE-75120 Uppsala, Sweden*

Neural quantum states (NQS) attract a lot of attention due to their potential to serve as a very expressive variational ansatz for quantum many-body systems. Here we study the main factors governing the applicability of NQS to frustrated magnets by training neural networks to approximate ground states of several moderately-sized Hamiltonians using the corresponding wavefunction structure on a small subset of the Hilbert space basis as training dataset. We notice that generalization quality, i.e. the ability to learn from a limited number of samples and correctly approximate the target state on the rest of the space, drops abruptly when frustration is increased. We also show that learning the sign structure is considerably more difficult than learning amplitudes. Finally, we conclude that the main issue to be addressed at this stage, in order to use the method of NQS for simulating realistic models, is that of *generalization* rather than *expressibility*.

Following fascinating success in image and speech recognition tasks, machine learning (ML) methods have recently been shown to be useful in physical sciences. For example, ML has been used to classify phases of matter [1], to enhance quantum state tomography [2, 3], to bypass expensive dynamic ab initio calculations [4], and more [5]. Currently, artificial neural networks (NNs) are being explored as variational approximations for many-body quantum systems in the context of variational Monte Carlo (vMC) approach. vMC is a well-established class of methods suitable for studying low-energy physics of many-body quantum systems with a more than fifty-year history [6]. A vast variety of trial wave functions have been suggested in different contexts. One of the simplest choices is mean-field form of the wavefunction which can be enriched by explicit account for particle-particle correlation [7–9] and generalized to include many variational parameters [10–13]. Certain tensor network variational ansätze, e.g. Matrix Product States [14], do not require stochastic Monte Carlo sampling and are thus amenable to exact optimization. The common shortcoming of all these methods is that the trial functions are tailored to a concrete model of interest and often require some prior knowledge about structure of the ground state (such as short-range entanglement for MPS methods) or intuition which helps constrain the optimization landscape (e.g. approximate understanding of nodal surfaces for Quantum Monte Carlo methods [15]). However, in many cases our prior intuition can be insufficient or unreliable. This poses a natural question whether a more generic ansatz that can efficiently approximate ground

states of many-body systems could exist.

A novel and fresh look at this problem was given in [16], where the traditional vMC optimization approach was hybridized with ML. A simple yet very unrestricted variational ansatz that inherits the structure of a certain neural network – Restricted Boltzmann Machine (RBM) was suggested. For the test cases of one- and two-dimensional Heisenberg and transverse field Ising models, it was demonstrated that, optimizing this ansatz with the Stochastic Reconfiguration (SR) scheme [17], one could achieve high accuracy in approximating ground states of systems of up to hundreds of spins, sometimes outperforming the state-of-the-art methods.

In subsequent years, a number of new variational neural quantum states have been suggested and their properties were thoroughly analyzed. Among other important discoveries, it was realized that even the simplest RBMs with polynomial number of parameters have rich enough structure to host volume law entanglement [18, 19], indicating that NQS are more flexible than, for instance, tensor networks [20]. Recently, RBM representation for open quantum systems has been formulated [21–23]. Hybrid wave functions, combining properties of RBMs and more traditional pair product wave functions, were demonstrated to significantly reduce relative energy error of variational ground state of two-dimensional Fermi-Hubbard model [24] and to enhance the accuracy of Gutzwiller-projected wave functions in frustrated magnets [25]. An algorithm for computing the spectrum of low-lying excited states has been suggested [26], opening a route to studying finite-temperature phenomena with

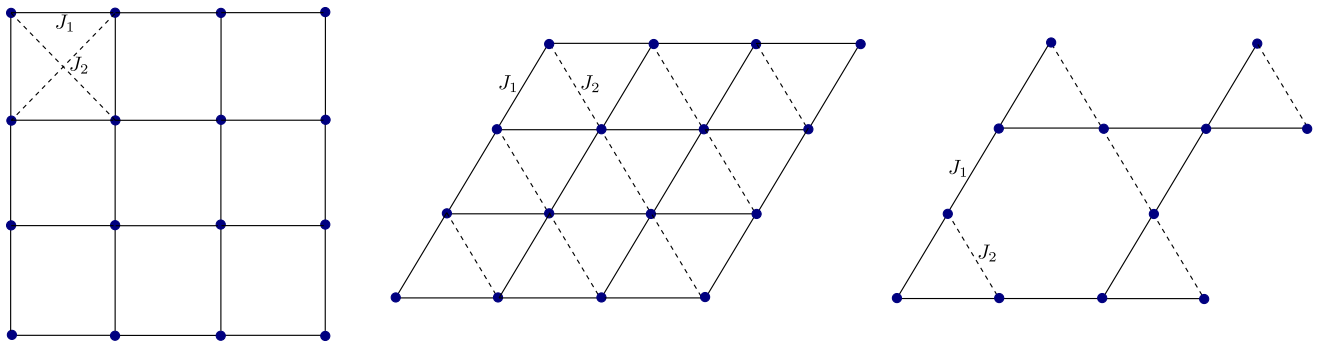


FIG. 1. The three studied cases of the frustrated antiferromagnetic Heisenberg model: next-nearest neighbor $J_1 - J_2$ model on a square lattice (left), nearest-neighbor model on an anisotropic triangular lattice (middle), spatially anisotropic Kagome lattice (right). In all cases $J_2 = 0$ corresponds to the absence of frustrations.

NQS (see also [27]). However, it also became evident that NQS must not be perceived as a magic bullet in the area of strongly correlated quantum systems [28]. Although a variational wave function with a network structure may be able to approximate the ground state really well, in some cases the desired point in the space of variational parameters can be hard to reach, and learning algorithm hits a saddle point before approaching the solution. This results in a large relative energy error and a low overlap between the NQS and the actual exact ground state, making the obtained solution almost useless for computing physical observables. This problem is particularly pronounced for systems where the energy gap between the ground state and the first excited state is very small, like for frustrated spin systems such as $J_1 - J_2$ antiferromagnetic Heisenberg model on square lattice [29], or the Fermi-Hubbard model away from the neutrality point [30].

An important feature of any ansatz is its *expressibility*, – a potential capacity to represent a many-body wave function with high accuracy using a moderate number of parameters¹ [32–34], and so far, significant effort has been put into the search for neural quantum states architectures that possess this property [3, 35]. At the same time, there is another issue that is not widely discussed in this context, – the *generalization* properties of an ansatz. To illustrate this aspect, it is instructive to consider the problem of fitting a known wavefunction by a certain ansatz. For a sufficiently large quantum system, even evaluation of the cost function (which depends on the ansatz parameters and measures the fit quality) and its gradients may become impossible as it requires summing over a very large number of terms in the Hilbert space. One may hope that, by instead evaluating the cost func-

tion on a smaller set of the Hilbert space basis, sampled in a certain way, one will eventually approach point of optimality close to the actual solution of the full optimization problem. This is not guaranteed at all, and is exactly what is known as generalization property in the ML context. This issue is also very important in the variational optimization scheme. In vMC, an ansatz is adjusted iteratively in a certain way, so that it is expected that the system ends up in the lowest energy state allowed by the form of the ansatz [17, 36, 37]. At each step of this iterative procedure, one has to evaluate the change of the trial wavefunction parameters. This relies on MC sampling from basis of the Hilbert space of the model, and for large systems the total number of samples is negligibly small in comparison with the dimension of the Hilbert space. Hence, it is of crucial importance for the ansatz to accurately generalize onto a larger subspace that was not sampled in the course of learning and correctly estimate phases and amplitudes of the wavefunction on the full set of basis vectors. Although generalization properties of neural networks have been analyzed [38, 39] in more conventional machine learning context, we are not aware of any systematic studies of this issue for the problem at hand — approximating the eigenstates of large quantum systems, — and with the present work we fill this gap.

Although the generalization issue concerns both phases and amplitudes of the wavefunction coefficients, it turns out that these two components behave differently in this respect. Already from the first works in the field, it seemed plausible that effectiveness of NN as variational ansatz is somehow connected to the sign structure of the models. For instance, in [16], even for the unfrustrated Heisenberg antiferromagnet on a square lattice, the Hamiltonian must first be brought into stoquastic (sign-definite) form by a unitary transformation in order to reduce noise and attain proper level of convergence (see also [40]). As another example, let us note that in recent study [37] it was stressed that biasing the NQS ansatz with certain predefined (heuristic) sign structures

¹ It can be proven mathematically that NNs can in principle approximate any smooth function to arbitrary accuracy [31], but it might require an impractically large number of parameters.

is very important for performance of the method. Therefore, although we will study both aspects, special attention will be paid to the sign structure.

We consider several antiferromagnetic spin models described by the Heisenberg Hamiltonian:

$$\hat{H} = J_1 \sum_{\langle a,b \rangle} \hat{\sigma}_a \otimes \hat{\sigma}_b + J_2 \sum_{\langle\langle a,b \rangle\rangle} \hat{\sigma}_a \otimes \hat{\sigma}_b, \quad (1)$$

where, for each lattice geometry, the first sum is taken over the unfrustrated sublattice (solid lines in Fig. 1), and the second sum is taken over the sublattice that brings in frustrations (dashed lines in Fig. 1). Namely, we consider $J_1 - J_2$ model on a square lattice [41–43] and the nearest-neighbor antiferromagnets on spatially anisotropic triangular [44] and Kagome [45, 46] lattices. These models are known to host spin liquid phases in certain domains of J_2/J_1 , to which we further refer as frustrated regions.

For every model, its ground state belongs to the sector of minimal magnetization, thus the dimension of the corresponding Hilbert space is $K = C_{[N/2]}^N$ (where N is the number of spins). It is convenient to work in the basis of eigenstates of $\hat{\sigma}^z$ operator: $|\mathcal{S}\rangle \sim |\uparrow\downarrow \dots \downarrow\uparrow\rangle$. In this basis the Hamiltonian \hat{H} is real-valued. The ground state is thus also real-valued, and every coefficient in its basis expansion is characterized by a sign $s_i = \text{sign}(\psi_i)$ (instead of a continuous phase):

$$|\Psi_{GS}\rangle = \sum_{i=1}^K \psi_i |\mathcal{S}_i\rangle = \sum_{i=1}^K s_i |\psi_i| |\mathcal{S}_i\rangle. \quad (2)$$

By running numerical experiments, we shall demonstrate that it is indeed the lack of sign structure generalization that prevents a neural quantum state from learning the wavefunction, even though expressibility of the corresponding ansatz could be good enough. First, we solve each of the models using exact diagonalization. Then, with the exact ground state as a target, we use supervised learning to train the NQS. During the training procedure, NNs are shown only a tiny fraction of the ground state (which is chosen by sampling from the probability distribution $\propto |\psi_i|^2$). Quality of the approximation is then assessed on the remaining part of the Hilbert space basis which we call *test dataset*. We tune both the training dataset size as well as the degree of frustration (controlled by J_2/J_1), and show that when the models are interpolated between unfrustrated and fully frustrated regimes, networks’ generalization abilities change in a non-trivial way, with sign structure becoming very difficult to learn in certain cases. This motivates a search for neural quantum states architectures which generalize better.

RESULTS

We have analyzed how NNs learn ground state structures of three lattice models. In what follows, we will be mainly speaking about periodic clusters of 24 spins, since all the effects are clear already in that case, but will also provide results for 30-spin clusters, and some data for a 6-by-6 periodic square lattice. Effective dimension of a 24-spin system Hilbert space in the zero-magnetization sector is $d = C_{12}^{24} \simeq 2.7 \cdot 10^6$. Our main results seem universal for all studied models and architectures and can be summarized in the following four statements.

- (i) Generalization from a relatively small subset of Hilbert space basis of the wavefunction sign structure is not granted even when the ansatz is able to express the ground state with high accuracy. Very well known to machine learning practitioners, this fact is also valid for spin systems, in both frustrated and ordered regimes.
- (ii) Construction and training of a network to achieve good generalization, a task which is relatively simple in the ordered phase, becomes much harder upon approaching the frustrated regime.
- (iii) Quality of generalization depends on the size of training set in an abrupt way exhibiting a sharp increase at some $\varepsilon_{\text{train}} = \frac{\text{training dataset size}}{\text{Hilbert space dimension}}$.
- (iv) Generalization of wave function amplitudes turns out to be a substantially easier task than generalization of signs.

In the remaining part of this section we explain the findings in more detail using Kagome lattice as an example. We focus on a two-layer dense neural network architecture. For results for other models and detailed comparison of different architectures we refer the reader to Supplementary Material.

Upper row on Fig. 2 illustrates both points **i** and **ii**. Here, we use a small subset (1%) of the Hilbert space basis to train the NN and then evaluate how well it predicts the sign structure on the remaining basis vectors unavailable to it during training. To assess the quality of generalization we use overlap between the exact ground state and the trial state. The latter is defined as a state with amplitudes taken from exact diagonalization and sign structure encoded in a NN (the sign is chosen by following the most probable outcome according to the NN). Consider, for example, the right panel, where generalization quality for Kagome model is shown as a function of J_2/J_1 . It is known [46] that Kagome model hosts a frustrated regime for $0.51 \lesssim J_2/J_1 \lesssim 1.82$. Strikingly, this phase transition shows itself as a sharp decrease of overlap around the value $J_2/J_1 \approx 0.51$. As one may expect, the frustrated regime is characterized

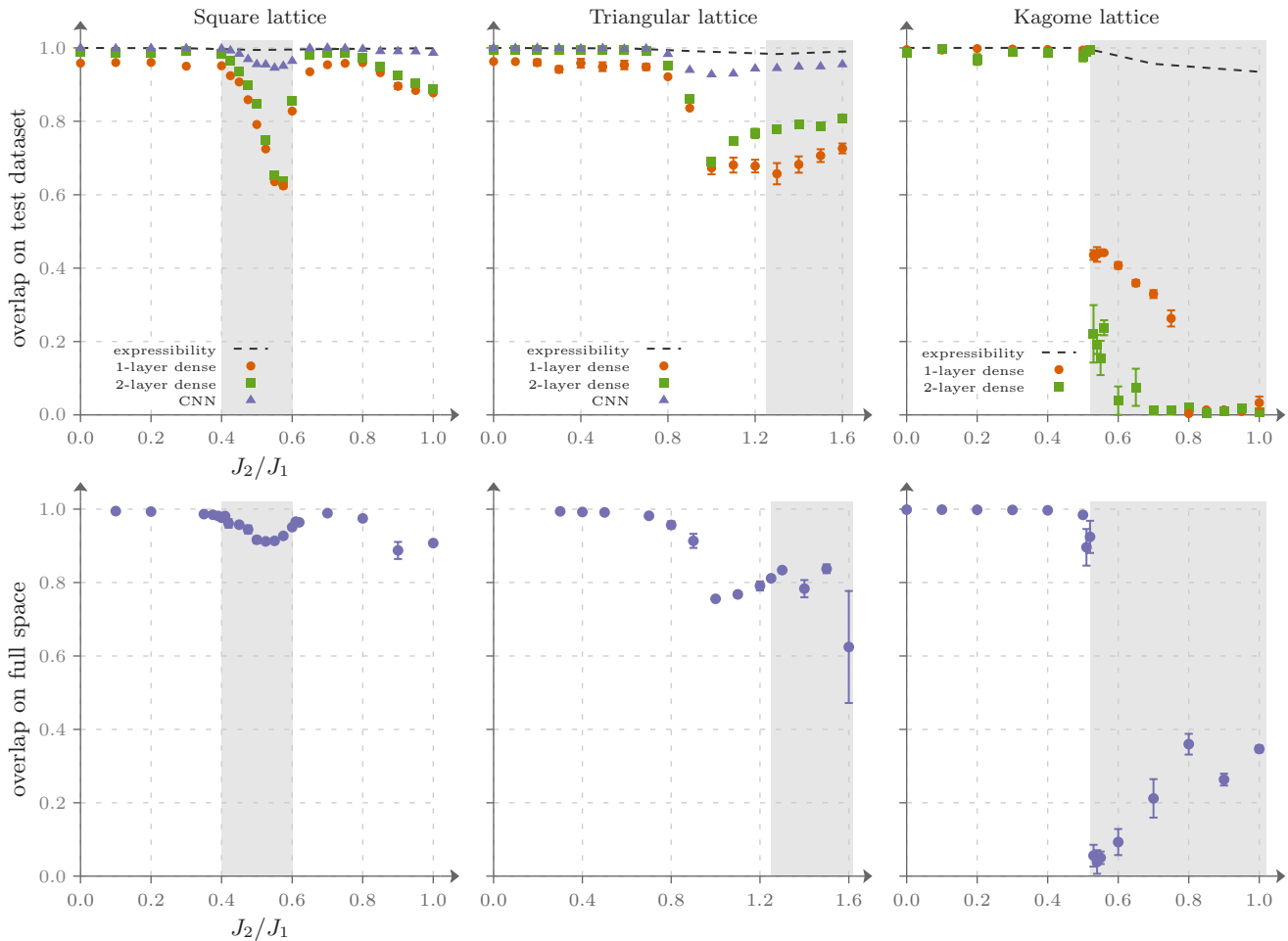


FIG. 2. Upper row: Overlap of the variational wave function with the exact ground state as a function of J_2/J_1 computed for the square (left), triangle (center) and Kagome (right) lattices. Overlap is computed on the test dataset (not included into training and validation datasets). Note that generalization is poor in the frustrated regions (which are shaded on the plots). NN architectures are described in Supplemental Material. Bottom row: quality of Stochastic Reconfiguration measured by overlap between the variational wave function and the exact ground state for systems of 24 spins (2-layer dense network is used). A correlation between generalization quality and accuracy of the SR method is evident. On this figure, as well as on all the subsequent ones (both in the main text and Supplemental Material), error bars represent standard error (SE) obtained by repeating simulations multiple times.

by very intricate sign distribution leading to a drastic reduction in the overlap. For the square and the triangular lattices (left and middle panels of Fig. 2), generalization quality behaves somewhat differently. For $J_1 - J_2$ model on the square lattice, instead of a sharp transition, it exhibits a large but smooth dip in frustrated regime ($0.4 < J_2/J_1 < 0.6$). On the triangular lattice, the minimum is reached slightly before approaching the transition point ($J_2/J_1 \approx 1.25$). However, for all three models we see that behavior of generalization quality reflects very well the known phase transitions with generalization being easy in ordered phases and becoming notoriously hard in disordered phases. Note also that different neural networks may generalize very differently: in particular, as

shown for the square and triangular lattices of Fig. 2, dips in performance of convolutional NNs are much smaller than for dense networks. Such good performance is most likely due to the fact that our implementation of CNNs accounts for translational symmetry (see Supplementary Material for an in-depth explanation of used NN architectures).

We believe that experiments of this kind would help to choose proper architectures to be used in vMC methods such as SR. In Stochastic Reconfiguration scheme, parameter updates are calculated using a small (compared to the Hilbert space dimension) set of vectors sampled from the probability distribution proportional to $|\psi|^2$. This closely resembles the way we choose our training

dataset. Moreover, SR does not optimize energy directly, rather at each iteration it tries to maximize the overlap between the NQS $|\Psi\rangle$ and the result of its imaginary time evolution $(1 - \delta t \hat{H})|\Psi\rangle$. Hence, even though our supervised learning scheme and SR differ drastically, their efficiencies are strongly related. To make this correlation more apparent, we have performed several vMC experiments for 24-spin clusters. In the second row of Fig. 2, we provide results of SR simulations for different values of J_2/J_1 . One can see that the two learning schemes follow very similar patterns.

Let us now turn to observation iii. As we have already mentioned, it is very important to distinguish the ability to represent the data from generalization. In the context of NQS, the former means that a NN is able to express complex quantum states well if training was conducted in a perfect way. For clusters of 24 spins² we have trained the networks on the entire ground state and found that expressibility of the ansätze is not an issue, – we could achieve overlaps above 0.94 for all values of J_2/J_1 (Dashed lines in the upper row of Fig. 2). However, this ability does not automatically make a neural network useful if it cannot generalize well. To make the boundary more clear, we study how generalization quality changes when size of the training dataset is increased. Results for Kagome lattice are shown on the Fig. 3. Interestingly, even in the frustrated regime ($J_2 = 0.6$) it is possible to generalize reasonably well from a relatively small subset of the basis states, but the required $\varepsilon_{\text{train}}$ becomes substantially larger than in the magnetically ordered phase. Most importantly, the ability of the NN to generalize establishes in an abrupt manner contrary to more typical smooth behavior observed in statistical models of learning [47–49]. Another interesting feature is saturation of the overlap at large $\varepsilon_{\text{train}}$ which can be observed in larger systems³, see Fig. S5 and S7.

In our discussion up to this point, we concentrated entirely on the quality of generalization of the wavefunction sign structure. One may wonder whether it is indeed the signs rather than amplitudes which are responsible for the difficulty of learning the wavefunction as a whole (this possibility has been discussed in the context of state tomography in [2]). To prove this statement, we conduct the following analysis. In the context of learning, overlap between a trial wavefunction and the target state can be used to characterize the effectiveness of NNs in two different ways. First, one can fix the amplitudes of the

wavefunction and use a NN to learn the signs. This produces a trial wavefunction ψ_{sign} . Alternatively, one can fix the sign structure, and encode the amplitudes in a NN to get a trial wavefunction ψ_{amp} . Clearly, the accuracy of ψ_{amp} and ψ_{sign} will depend on the relative complexity of learning amplitudes and signs of the wavefunction coefficients. We illustrate statement iv with Fig. 5, where we use overlap to compare the quality of generalization of signs and amplitudes (using, again, 1% of the basis for training). Upon increase of J_2 , one moves from a simple ordered phase to frustrated regime where overlap drops sharply. Although the generalization of both signs and amplitudes becomes harder at the point of phase transition $J_2/J_1 = 0.51$, drop in the sign curve is much larger, and at even higher J_2 the quality of the learned states becomes too poor to approximate the target wavefunction. At the same time, even deeply in the frustrated regime generalization of amplitudes, given the exact sign structure, leads to a decent result. Moreover, generalization quality of amplitudes does not drop abruptly when $\varepsilon_{\text{train}}$ is decreased, remaining non-zero on very small datasets (see Fig. S3). These observations suggest that it is indeed the sign part of the wavefunction that becomes problematic for generalization in frustrated region⁴.

So far we have been exemplifying our results on 24-spin clusters, and it is interesting to see whether the main observations hold for larger Hilbert spaces as well. Most of the computations that we performed can be repeated for lattices of 30 spins. Even bigger systems become too resource demanding and require a more involved algorithm implementation. Nevertheless, for the square lattice of 36 spins (6-by-6), we managed to compute dependency of generalization on the training dataset size for several values of J_2/J_1 . For the detailed analysis of 30-spin clusters we refer the reader to Supplemental Material. One can see that all the conclusions remain valid, – behavior of the generalization quality as function of J_2/J_1 is very similar to that for 24-spin clusters, and the dependence on $\varepsilon_{\text{train}}$ exhibits a sharp transition.

What is especially interesting is that the critical size of the training dataset required for non-zero generalization seems to scale relatively slowly with the system size. In Fig. 4, for the case of the square lattice, we show the critical size of the training dataset as a function of the Hilbert space dimension K . It turns out, that when one goes from 24 spins ($K \simeq 2.7 \cdot 10^6$) to 36 spins ($K \simeq 9 \cdot 10^9$), it is sufficient to increase the training dataset just by a factor of 10. This gives us hope that reasonable general-

² We believe that this result holds true for larger clusters. Unfortunately, we could not verify this: for 30 spins (Hilbert space dimension $\sim 1.5 \cdot 10^8$) training the network on the entire set of basis vectors is too resource-demanding.

³ It is hard to see this plateau in the system of 24 spins as it requires too large $\varepsilon_{\text{train}}$, such that all relevant basis vectors end up in the training dataset, and overlap computed on the rest of the basis is meaningless.

⁴ Bear in mind that difficult to learn sign structure is not directly related to the famous Quantum Monte Carlo sign problem. For example, Fig. 2 shows that in $J_2 \rightarrow 0$ limit of J_1 - J_2 model, networks have no trouble learning the sign structure even though in $\hat{\sigma}^z$ basis, there is sign problem since we are not applying Marshall’s Sign Rule.

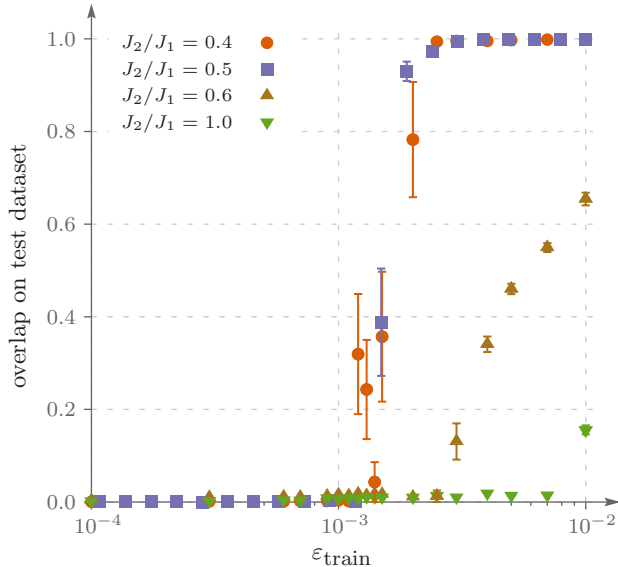


FIG. 3. Dependence of generalization quality on the size of the training data set ϵ_{train} for Kagome model for $J_2/J_1 = 0.4, 0.5, 0.6, 1.0$. It is measured by overlap between the variational and the exact states computed on the test dataset.

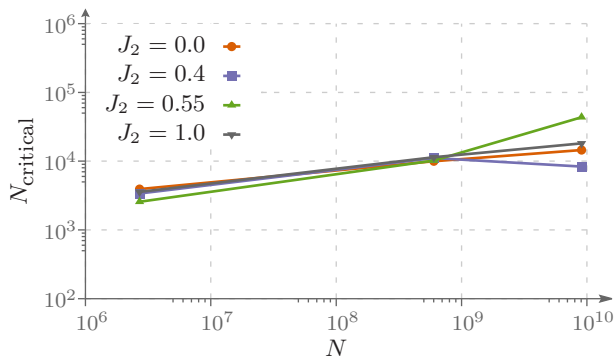


FIG. 4. Critical size of the training dataset (which is required for non-zero generalization) as a function of the Hilbert space dimension. One can see that it scales relatively slowly.

ization quality can be achieved for even larger systems.

DISCUSSION

In this paper, we have analyzed the ability of neural networks to generalize many-body quantum states from a small number of basis vectors to the whole Hilbert space. The main observation we made is that for all models we have considered, quality of generalization of the ground state sign structure falls off near quantum phase transitions and remains low in the frustrated regimes.

We have demonstrated that generalization may indeed be an essential factor that is likely responsible for spoiling

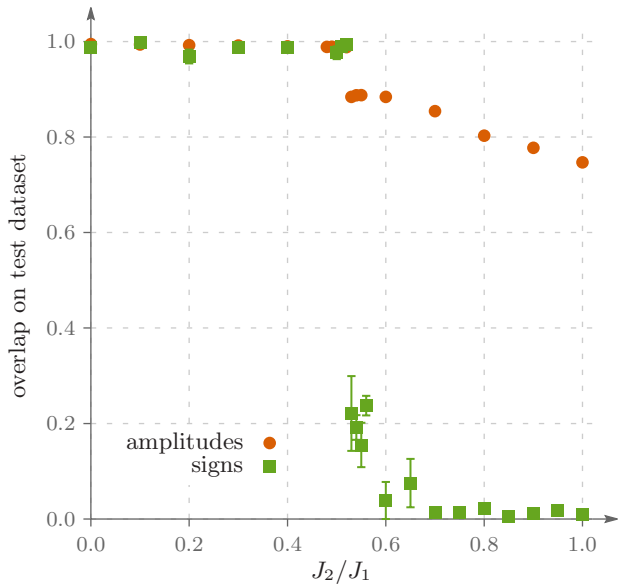


FIG. 5. Comparison of generalization quality as measured by overlap for learning the sign structure (red) and amplitude structure (green) for Kagome lattice for 2-layer dense architecture. Note that both curves decrease in the frustrated region, but sign structure is much harder to learn.

ing the convergence of NQS in a number of physically interesting cases such as frustrated quantum spin systems. Our main conclusion which is qualitatively valid for all the studied models and NN architectures is that a NN struggles to *generalize* the distribution of signs in the ground state of a many-body system with competing interactions in the regime of strong frustrations if the training is done on a small fraction of basis states. At the same time, even simple neural networks seem to have no problem in generalizing amplitudes from the training dataset onto the entire Hilbert space, and have very good capacity to *express* both sign and amplitude distributions of the studied states. Hence, in a search for neural quantum state architectures that can be trained to approximate the ground state of a large-scale many-body Hamiltonian, one should mainly focus on NNs that are at least capable of generalizing the ground state sign structure of moderately-sized test systems. At this point, it is hard to give a concrete recipe of how to look for such architectures, but one of the possible ways could be to incorporate symmetries of the system into the network structure (improving the learning protocols may also help [50]). In our examples, using convolutional NNs that respected translational symmetries of the square and triangular lattices helped improve generalization quality significantly. This also suggests that our results are heuristic: although we have studied several most popular NN architectures, we can not exclude a possibility that for certain other designs, the generalization will show features, qualitatively different from our findings.

Another important feature we have discovered is the threshold behavior of generalization as a function of the training dataset size. This is rather unusual and different from the smooth behavior known for standard models of learning, such as teacher-student scenario in a binary perceptron [47, 48] and some other studies of NNs generalization [51]. From the point of view of vMC applications, it is desirable to understand how the required number of samples depends on system parameters such as size and degree of frustration and training algorithm parameters.

As a closely related phenomenon, let us mention the fact known from the binary perceptron problem: bias towards dense clusters of local minima on the loss landscape makes generalization error a significantly steeper function of the number of the samples [49]. This may partially explain the observed abrupt change in generalization quality since stochastic gradient descent employed by us is known to have similar properties (bias towards wide minima of the loss landscape [39, 52, 53]). It would be very useful to have analytically tractable models which show the threshold behavior of generalization.

Finally, it is worth mentioning that, while the dip in generalization is not desirable in the context of variational energy optimization, it could be used as a tool to identify – in a completely unsupervised manner – the position of the phase transitions, similarly in spirit to approaches of [54–57].

METHODS

In this study, we use feed-forward networks of three different architectures (dense 1-layer, dense 2-layer, and convolutional 2-layer) to encode wavefunction coefficients via splitting them into amplitudes and signs. All of our networks have the same input format: spin configuration $|\mathcal{S}_i\rangle = |\sigma_1\sigma_2\dots\sigma_N\rangle$ represented as a binary sequence, $\sigma_k = \pm 1$. Network encoding amplitudes outputs a real number, – natural logarithm of the amplitude. Network encoding sign structure outputs a probability $p \in [0, 1]$ for the corresponding sign to be plus. For inference we then use “+” whenever $p \geq 0.5$ and “–” otherwise. Thus, unlike the approach of [16], we represent wavefunction signs using a binary classifier.

Both networks are trained on data obtained from exact diagonalization. We sample $\varepsilon_{\text{train}} \cdot K$ spin configuration from the Hilbert space basis according to probability distribution $P(i) = \frac{|\psi_i|^2}{\sum_j |\psi_j|^2}$. They constitute the training dataset⁵. Then, we sample another $\varepsilon_{\text{val}} \cdot K$

spin configurations which we use as a validation dataset during training. It enables us to monitor the progress and employ regularization techniques such as early stopping. In practical applications of NQS [16, 26, 29], SR [17, 58], Stochastic Gradient Descent [12, 59], or Generalized Lanczos [36], the training dataset is generated by Monte Carlo sampling from basis of the Hilbert space of the model, and, since dimension of the latter grows exponentially with the number of spins, only a tiny fraction of it can be covered with a Monte Carlo chain in reasonable time. Therefore it is natural to mimic this incomplete coverage with $\varepsilon_{\text{train}}, \varepsilon_{\text{val}} \ll 1$.

To assess the performance of the NNs we evaluate overlap (scalar product) between exact eigenstate and the trial state. A trial state for sign NN is defined as a state with amplitudes from ED and sign structure encoded in a NN. Analogously, a trial state for amplitude NN is obtained by superimposing the exact sign structure onto the positive amplitudes encoded in the amplitude NN.

We train the classifier by minimizing *binary cross-entropy loss function*

$$\mathcal{L}^S = - \sum_i \left(\frac{1+s_i}{2} \log p_i + \frac{1-s_i}{2} \log(1-p_i) \right), \quad (3)$$

where p_i is the predicted probability for the spin configuration $|\mathcal{S}_i\rangle$ to have sign +1, $s_i = \pm 1$ is the expected sign obtained from ED, and the sum is taken over the training dataset.

Training of the neural network which approximates amplitudes occurs via minimization of

$$\mathcal{L}^A = \sum_i (\log |\psi_i| - \log |\psi_i^e|)^2, \quad (4)$$

where ψ_i^e is the exact value of i -th coefficient.

Usually, in machine learning algorithms it is crucial to choose hyperparameters correctly. For example, dependence of critical $\varepsilon_{\text{train}}$ on batch size is non-monotonic. Choosing a wrong batch size can lead to an order of magnitude increase of required $\varepsilon_{\text{train}}$. In our calculations, we typically work with batches of 64 or 128 samples. For optimization, we mostly use Adam [60] (a stochastic gradient-based method) with learning rates around $10^{-4} - 10^{-3}$. Early stopping is our main regularization technique, but we have also experimented with dropout layers (which randomly throw away some hidden units) and L_2 -regularization. Code to reproduce our results and more details about the training scheme can be found on GitHub [61, 62].

it is essential to correctly predict signs in front of basis vectors with large amplitudes. At the same time, incorrectly guessing signs corresponding to spin configurations with small amplitudes leaves overlap of the variational wavefunction with the exact ground state intact.

⁵ Another option would be to sample the training dataset uniformly. However, we stick to sampling from probability distribution $P(i)$ because it produces better results and, intuitively,

ACKNOWLEDGMENTS

We are thankful to Dmitry Ageev and Vladimir Mazurenko for collaboration during the early stages of the project. We have significantly benefited from encouraging discussions with Giuseppe Carleo, Juan Carrasquilla, Askar Iliasov, Titus Neupert, and Slava Rychkov. The research was supported by the ERC Advanced Grant 338957 FEMTO/NANO and by the NWO via the Spinoza Prize. The work of A.A.B. which consisted of designing the project (together with K.S.T.), implementation of prototype version of the code, and providing general guidance, was supported by Russian Science Foundation, Grant No. 18-12-00185. The work of N.Yu.A. which consisted of numerical experiments, was supported by the Russian Science Foundation Grant No. 16-12-10059. N.Yu.A. acknowledges the use of computing resources of the federal collective usage center Complex for Simulation and Data Processing for Mega-science Facilities at NRC Kurchatov Institute, <http://ckp.nrcki.ru/>. K.S.T. is supported by Alexander von Humboldt Foundation and by the program 0033-2019-0002 by the Ministry of Science and Higher Education of Russia.

* t.westerhout@student.science.ru

† nikita.astrakhantsev@phystech.edu

‡ tikhonov@itp.ac.ru

§ m.katsnelson@science.ru.nl

¶ a.bagrov@science.ru.nl

- [1] J. Carrasquilla and R. G. Melko, *Nature Physics* **13**, 431 (2017).
- [2] G. Torlai, G. Mazzola, J. Carrasquilla, M. Troyer, R. Melko, and G. Carleo, *Nature Physics* **14**, 447 (2018).
- [3] D. Sehayek, A. Golubeva, M. S. Albergó, B. Kulchytskyy, G. Torlai, and R. G. Melko, *Physical Review B* **100**, 195125 (2019).
- [4] F. Brockherde, L. Vogt, L. Li, M. E. Tuckerman, K. Burke, and K.-R. Müller, *Nature Communications* **8**, 872 (2017).
- [5] G. Carleo, I. Cirac, K. Cranmer, L. Daudet, M. Schuld, N. Tishby, L. Vogt-Maranto, and L. Zdeborová, *Rev. Mod. Phys.* **91**, 045002 (2019).
- [6] W. L. McMillan, *Physical Review* **138**, A442 (1965).
- [7] C. Gros, D. Poilblanc, T. Rice, and F. Zhang, *Physica C: Superconductivity* **153**, 543 (1988).
- [8] T. Giamarchi and C. Lhuillier, *Physical Review B* **43**, 12943 (1991).
- [9] G. Dev and J. Jain, *Physical Review B* **45**, 1223 (1992).
- [10] C. Umrigar and C. Filippi, *Physical Review Letters* **94**, 150201 (2005).
- [11] F. Schautz and C. Filippi, *The Journal of Chemical Physics* **120**, 10931 (2004).
- [12] A. Harju, B. Barbiellini, S. Siljamäki, R. M. Nieminen, and G. Ortiz, *Physical Review Letters* **79**, 1173 (1997).
- [13] M. Capello, F. Becca, M. Fabrizio, S. Sorella, and E. Tosatti, *Physical Review Letters* **94**, 026406 (2005).
- [14] F. Verstraete and J. I. Cirac, *Physical Review B* **73**, 094423 (2006).
- [15] J. B. Anderson, *International Reviews in Physical Chemistry* **14**, 85 (1995).
- [16] G. Carleo and M. Troyer, *Science* **355**, 602 (2017).
- [17] S. Sorella, M. Casula, and D. Rocca, *The Journal of Chemical Physics* **127**, 014105 (2007).
- [18] D.-L. Deng, X. Li, and S. D. Sarma, *Physical Review X* **7**, 021021 (2017).
- [19] Y. Levine, O. Sharir, N. Cohen, and A. Shashua, *Physical Review Letters* **122**, 065301 (2019).
- [20] R. Orús, *Annals of Physics* **349**, 117 (2014).
- [21] G. Torlai and R. G. Melko, *Physical Review Letters* **120**, 240503 (2018).
- [22] F. Vicentini, A. Biella, N. Regnault, and C. Ciuti, *Phys. Rev. Lett.* **122**, 250503 (2019).
- [23] M. J. Hartmann and G. Carleo, *Phys. Rev. Lett.* **122**, 250502 (2019).
- [24] Y. Nomura, A. S. Darmawan, Y. Yamaji, and M. Imada, *Physical Review B* **96**, 205152 (2017).
- [25] F. Ferrari, F. Becca, and J. Carrasquilla, *arXiv:1906.00463* (2019).
- [26] K. Choo, G. Carleo, N. Regnault, and T. Neupert, *Physical Review Letters* **121**, 167204 (2018).
- [27] N. Irikura and H. Saito, *arXiv:1911.02774* (2019).
- [28] C.-Y. Park and M. J. Kastoryano, *arXiv:1910.11163* (2019).
- [29] X. Liang, W.-Y. Liu, P.-Z. Lin, G.-C. Guo, Y.-S. Zhang, and L. He, *Physical Review B* **98**, 104426 (2018).
- [30] D. Luo and B. K. Clark, *Physical Review Letters* **122**, 226401 (2019).
- [31] K. Hornik, M. Stinchcombe, and H. White, *Neural networks* **2**, 359 (1989).
- [32] X. Gao and L.-M. Duan, *Nature Communications* **8**, 662 (2017).
- [33] Z. Cai and J. Liu, *Physical Review B* **97**, 035116 (2018).
- [34] G. Carleo, Y. Nomura, and M. Imada, *Nature Communications* **9**, 5322 (2018).
- [35] H. He, Y. Zheng, B. A. Bernevig, and G. Sierra, *arXiv:1910.13454* (2019).
- [36] S. Sorella, *Physical Review B* **64**, 024512 (2001).
- [37] K. Choo, T. Neupert, and G. Carleo, *arXiv:1903.06713* (2019).
- [38] G. Hinton and D. V. Camp, in *in Proc. of the 6th Ann. ACM Conf. on Computational Learning Theory* (ACM Press, 1993) pp. 5–13.
- [39] G. K. Dziugaite and D. M. Roy, *arXiv:1703.11008* (2017).
- [40] G. Torlai, J. Carrasquilla, M. T. Fishman, R. G. Melko, and M. Fisher, *arXiv:1906.04654* (2019).
- [41] H. Schulz, T. Ziman, and D. Poilblanc, *Journal de Physique I* **6**, 675 (1996).
- [42] J. Richter and J. Schulenburg, *The European Physical Journal B* **73**, 117 (2010).
- [43] H.-C. Jiang, H. Yao, and L. Balents, *Physical Review B* **86**, 024424 (2012).
- [44] S. Yunoki and S. Sorella, *Physical Review B* **74**, 014408 (2006).
- [45] A. P. Schnyder, O. A. Starykh, and L. Balents, *Physical Review B* **78**, 174420 (2008).
- [46] P. Li, R. Bishop, C. Campbell, D. J. Farnell, O. Götze, and J. Richter, *Physical Review B* **86**, 214403 (2012).
- [47] H. Sompolinsky, N. Tishby, and H. S. Seung, *Physical Review Letters* **65**, 1683 (1990).

- [48] H. S. Seung, H. Sompolinsky, and N. Tishby, *Physical Review A* **45**, 6056 (1992).
- [49] C. Baldassi, A. Ingrosso, C. Lucibello, L. Saglietti, and R. Zecchina, *Physical Review Letters* **115**, 128101 (2015).
- [50] R. Zen, L. My, R. Tan, F. Hebert, M. Gatto-bigio, C. Miniatura, D. Poletti, and S. Bressan, arXiv:1908.09883 (2019).
- [51] J. Langford and R. Caruana, in *Advances in Neural Information Processing Systems* (2002) pp. 809–816.
- [52] B. Neyshabur, S. Bhojanapalli, D. McAllester, and N. Srebro, in *Advances in Neural Information Processing Systems* (2017) pp. 5947–5956.
- [53] H. Li, Z. Xu, G. Taylor, C. Studer, and T. Goldstein, in *Advances in Neural Information Processing Systems* (2018) pp. 6389–6399.
- [54] E. P. Van Nieuwenburg, Y.-H. Liu, and S. D. Huber, *Nature Physics* **13**, 435 (2017).
- [55] P. Broecker, F. F. Assaad, and S. Trebst, arXiv:1707.00663 (2017).
- [56] W. Hu, R. R. Singh, and R. T. Scalettar, *Physical Review E* **95**, 062122 (2017).
- [57] E. V. Doggen, F. Schindler, K. S. Tikhonov, A. D. Mirlin, T. Neupert, D. G. Polyakov, and I. V. Gornyi, *Physical Review B* **98**, 174202 (2018).
- [58] M. Casula, C. Attacalite, and S. Sorella, *The Journal of Chemical Physics* **121**, 7110 (2004).
- [59] H. Saito and M. Kato, *Journal of the Physical Society of Japan* **87**, 014001 (2017).
- [60] D. P. Kingma and J. Ba, arXiv:1412.6980 (2014).
- [61] https://github.com/nikita-astronaut/nqs_frustrated_phase (2019).
- [62] <https://github.com/twesterhout/nqs-playground> (2019).

Supplemental Material

to the article “Neural Quantum States of frustrated magnets:
generalization and sign structure”

by T. Westerhout, N. Astrakhantsev, K. S. Tikhonov, M. I. Katsnelson
and A. A. Bagrov

In this Supplemental Material, we provide some additional information regarding the numerical analysis outlined in the main part of the paper.

I. NETWORK ARCHITECTURES

We use three different Neural Network architectures to demonstrate that the effects we observe might be general for all standard deep learning techniques.

a. One-layer dense network can be applied to all three models at hand. We arrange the spins in a linear pattern and feed them to the network which has one hidden layer of 64 neurons and the ReLU non-linearity. When it is used to approximate wavefunction amplitudes, only one output representing logarithm of the amplitude is taken. When it is used to learn the sign structure, it is equipped with two output nodes representing non-normalized probabilities of the sign to be ± 1 . Then, when the standard PyTorch cross entropy loss function is applied, those are converted into a single number $p \in [0, 1]$ with softmax. The total number of parameters in this network is $N \times 64 + 64 + 64 \times 2 = 1728$ (for 24 spins) or 2112 (for 30 spins).

b. Two-layer dense network can be applied to all three models at hand as well, and has a very similar structure as the one-layer one. Both hidden layers have 64 neurons. ReLU non-linearity is applied after every hidden layer. The total number of parameters is $N \times 64 + 64 + 64 \times 64 + 64 + 64 \times 2 = 5888$ (for 24 spins) or 6272 (for 30 spins).

c. CNN Periodic convolutional network can be applied to the J_1 - J_2 model on a square lattice. The main goal of this architecture is to preserve the translational invariance on the level of NN architecture. In every convolutional layer we apply periodic boundary conditions. When all the convolutional layers are applied, we take mean value operation over all spins in every “channel”, i.e. over all lattice sites. One can check that the prediction of such neural network is invariant with respect to any translation of the input spin configuration.

For the convolutional NN (CNN) architecture, we provide a listing of Python code using the PyTorch NN manipulation package. In what follows, the input parameter `is_odd` allows for selection between the momenta 0 and π in the y -direction. The goal of this architecture is to “hard-code” the translational invariance, i.e. if two outputs of the neural network mean probabilities of “+” and “-” signs, we would like them to remain unchanged in “even” case ($p_y = 0$) and exchange in the “odd” case ($p_y = \pi$) upon shift of the spin configuration in y direction. In order to achieve this property, the following procedure is performed. Before the action of every convolutional layer we periodically pad the input such that the valid convolution (convolving only the actual elements without going beyond the boundary) shrinks the configuration back to its initial size `x_size` \times `y_size`. After applying all the convolutional layers we perform weighted averaging over two spatial dimensions. All weights have the same absolute value and are all positive in the “even” case and have alternating signs in the “odd” case. The resulting vector of the length `n_channels` is mapped into one single number r by the dense layer without bias. This number has the property that it changes sign when the configuration is shifted in y -direction in the “odd” case and remains unchanged in the “even” case. It is then mapped onto two probabilities as $[p, 1 - p] = [\frac{1 + \tanh(r)}{2}, \frac{1 - \tanh(r)}{2}]$ which are then used to infer the sign of the configuration. It can be easily seen that the resulting probabilities are exchanged (and the sign is flipped in the “odd” case and remain intact in the “even” case upon the shift in y -direction), as required.

```
import torch

# 2D convolution preserving translational symmetry
class Conv2d(torch.nn.Module):
    def __init__(self, *args, **kwargs):
        super().__init__()
        self.conv = torch.nn.Conv2d(*args, **kwargs)

    def forward(self, x):
```

```

    # Periodic padding
    x = torch.cat([x, x[:, :, :, self.conv.kernel_size[0] - 1, :]], dim=2)
    x = torch.cat([x, x[:, :, :, :, self.conv.kernel_size[1] - 1]], dim=3)
    # Convolution + activation
    x = torch.relu(self.conv(x))
    return x

# Neural network predicting the sign structure.
class Net(torch.nn.Module):
    __constants__ = ["is_odd"]

    def __init__(self, is_odd=False):
        super().__init__()
        # Two convolutional layers
        self.conv1 = Conv2d(1, 32, kernel_size=5)
        self.conv2 = Conv2d(32, 64, kernel_size=5)
        # Final dense layer
        self.dense = torch.nn.Linear(64, 1, bias=False)

    def forward(self, x):
        x = x.view((x.size(0), 1) + self.size()[1:])
        # Convolutions
        x = self.conv1(x)
        x = self.conv2(x)
        # Enforcing translational symmetry by weighted averaging
        if self.is_odd:
            x[:, :, :, 2, :] *= -1
        x = x.mean(dim=(2, 3))
        # Final dense layer
        x = 0.5 * (1 + torch.tanh(self.dense(x)))
        # Returning probabilities
        return torch.cat([x, 1 - x], dim=1)

```

II. RESULTS OF ADDITIONAL NUMERICAL EXPERIMENTS

A. 24 spins

In this section, we provide some additional results for frustrated 24-spin clusters supporting the statements which we made in the main part of the paper. These results were obtained with two-layer dense network described in section I.

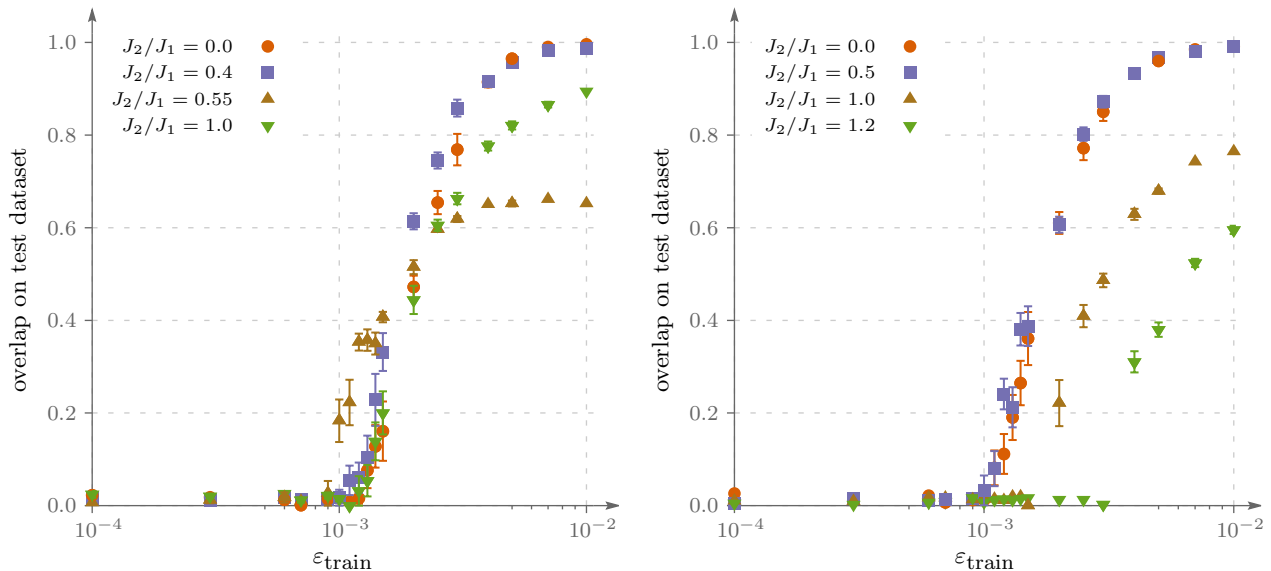


FIG. S1. Dependence of sign structure generalization quality on the size of the training dataset for square (left) and triangular (right) lattices.

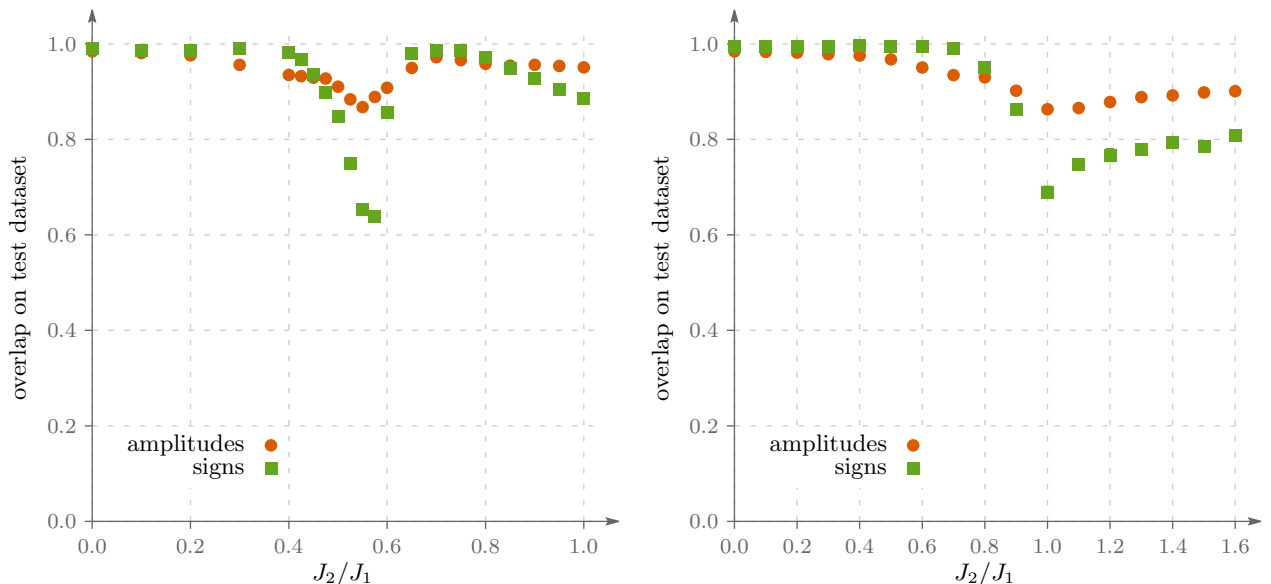


FIG. S2. Comparison of generalization quality for learning the sign structure (green) and amplitude structure (orange) for the square (left) and triangular (right) lattices.

In Fig. S1, we show the dependence of sign structure generalization quality on the training dataset size. We consider two lattices: square (left) and triangular (right). In both lattices, generalization quality exhibits a sharp transition

around certain critical value of $\varepsilon_{\text{train}}$. This is qualitatively the same as what we have observed for the Kagome lattice in the main text. It is interesting to note that for the square lattice, the transition occurs at the same $\varepsilon_{\text{train}}^*$ for different values of J_2/J_1 , while for the triangular and Kagome lattices $\varepsilon_{\text{train}}^*$ increases upon increasing the frustration.

In Fig. S2, we again show results for square and triangular lattices and highlight how difficult it is to generalize the sign structure compared to amplitude structure. Although for both learning tasks there is a dip in the generalization quality, it is evident that the sign structure is more difficult to learn in the frustrated regime.

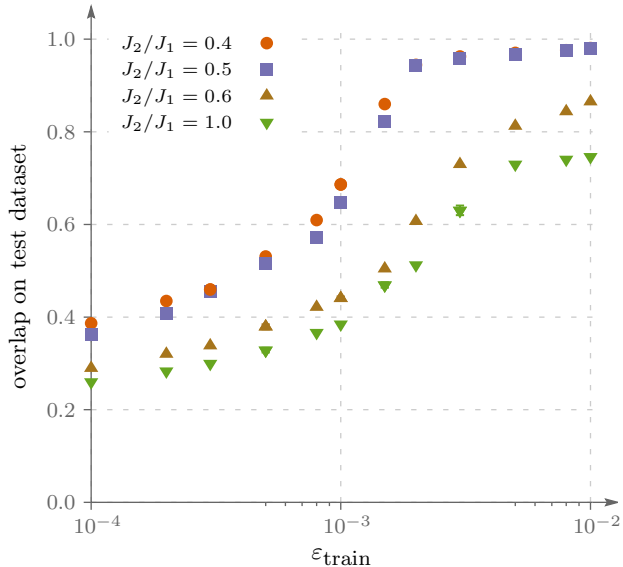


FIG. S3. Dependence of the amplitude value generalization quality on the training dataset size for Kagome lattice.

In Fig. S3, we show results for amplitude generalization quality dependence on $\varepsilon_{\text{train}}$, demonstrating that it exhibits smooth behavior in contrast with the one for the sign structure.

B. 30 spins

In this section, for the clusters of 30 spins we reproduce all the results that we obtained in the main text for 24-spin systems to demonstrate that our conclusions are valid for larger systems.

In Fig. S4, we plot the dependence of generalization quality on J_2/J_1 . Clearly, the patterns are very similar to what we have observed for clusters of 24 spins.

In Fig. S5, the abrupt improvement of generalization quality at some critical training dataset size $\varepsilon_{\text{train}}^*$ is shown. Comparing that to Fig. 3 in the main text, one can see that for larger systems a considerably smaller fraction of basis vectors is required for NN to start properly generalize the sign structure.

In Fig. S6, using the 2-layer dense neural network, we show that in the frustrated regime signs are more difficult to generalize than amplitudes.

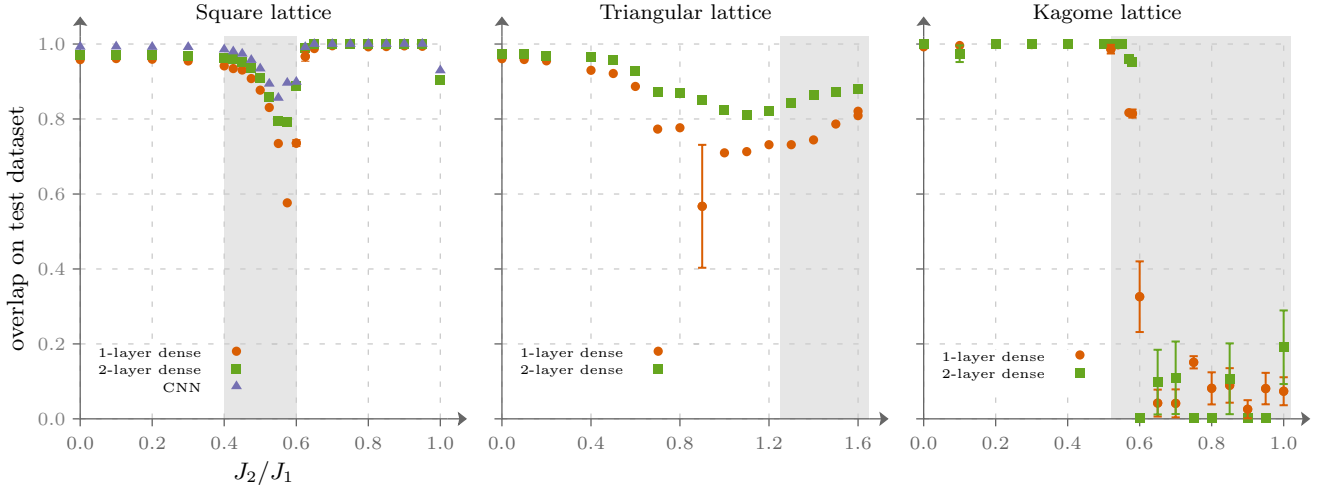


FIG. S4. Dependence of sign structure generalization quality (measured by overlap on the test dataset) on J_2/J_1 .

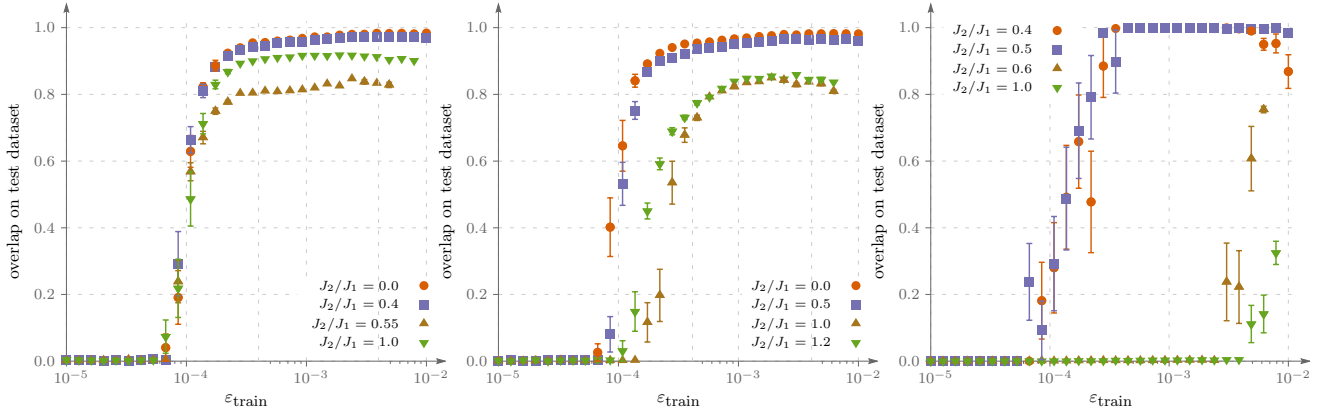


FIG. S5. Dependence of sign structure generalization quality on the size of the training dataset for three lattices: square (left), triangular (middle), and Kagome (right).

C. 32 & 36 spins

To estimate scaling of the critical training dataset size with system size (Fig. 4 of the main text), we have calculated ϵ_{train} -dependence of the sign structure generalization quality for the square lattice for even bigger systems. Fig. S7 shows results for 32- and 36-spin clusters.

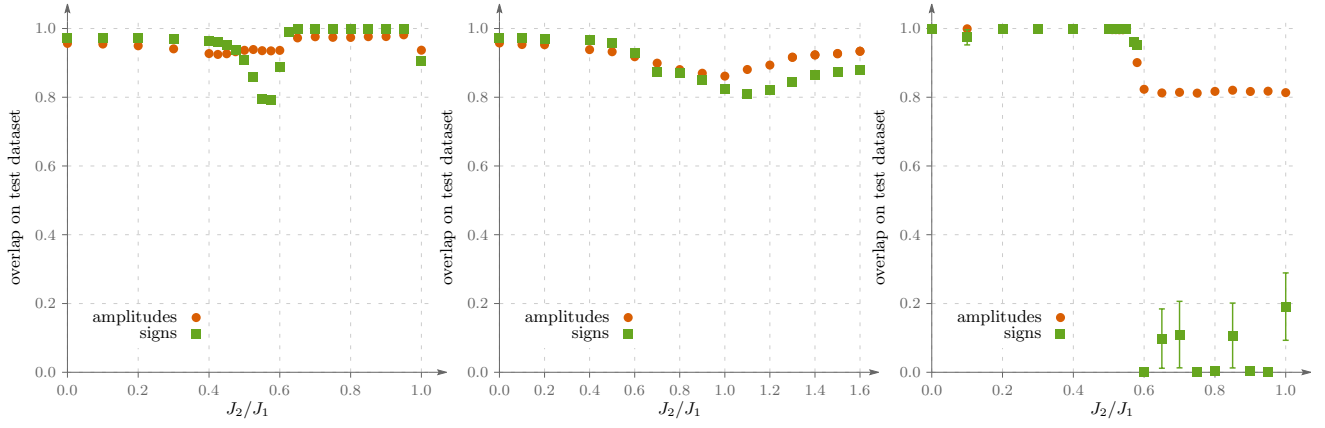


FIG. S6. Comparison of generalization quality for learning the sign structure (green) and amplitude structure (orange) for the J_1 - J_2 model on the square (left), triangular (middle), and Kagome (right) lattices with 2-layer dense architecture employed both for signs and amplitudes.

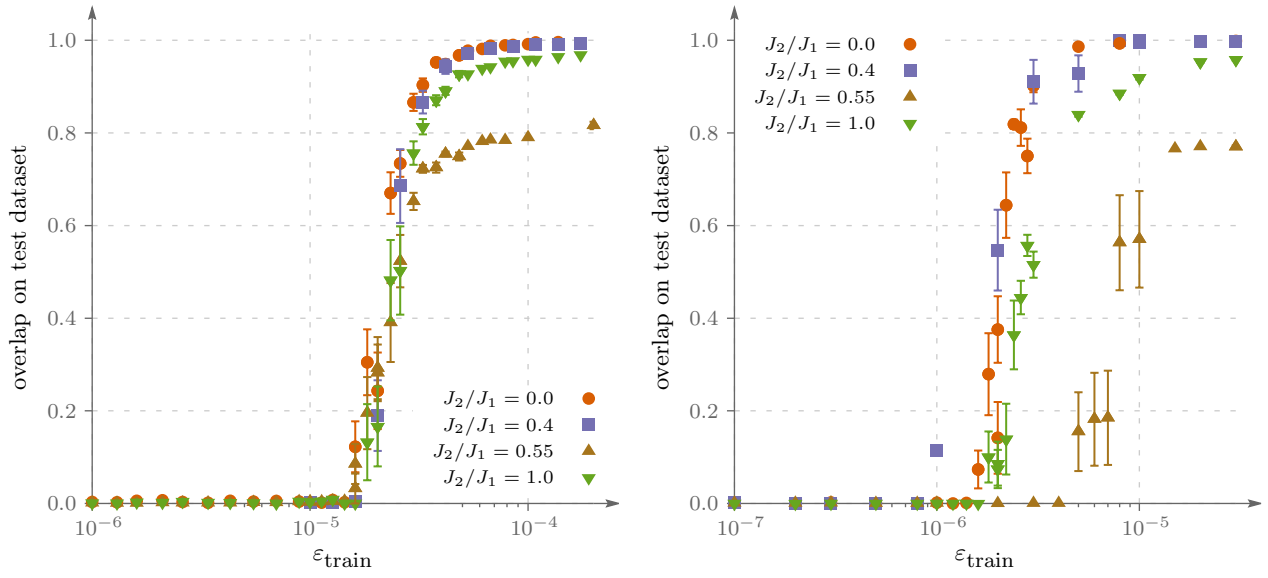


FIG. S7. Dependence of sign structure generalization quality on the size of the training data set ϵ_{train} for the J_1 - J_2 antiferromagnetic Heisenberg model on the square lattice with 32 (left) and 36 (right) spins.